Relative Stereochemistry and Absolute Configuration of Farinosin, a Eudesmanolide From *Encelia farinosa*

ALFREDO R. ORTEGA,[1] MARIANO SÁNCHEZ-CASTELLANOS,[1] NURY PÉREZ-HERNÁNDEZ,[2] RAMÓN E. ROBLES-ZEPEDA,[3] PEDRO JOSEPH-NATHAN,[4]* AND LEOVIGILDO QUIJANO[1]

[1]*Instituto de Química, Universidad Nacional Autónoma de México, Circuito Exterior, Ciudad Universitaria, Mexico City, Mexico*
[2]*Escuela Nacional de Medicina y Homeopatía, Instituto Politécnico Nacional, Mexico City, Mexico*
[3]*Departamento de Ciencias Químico Biológicas, Universidad de Sonora, Hermosillo, Sonora, Mexico*
[4]*Departamento de Química, Centro de Investigación y de Estudios Avanzados del Instituto Politécnico Nacional, Mexico City, Mexico*

ABSTRACT The naturally occurring eudesmanolide farinosin (**1**) is now fully characterized for the first time despite its original isolation almost half a century ago. The early assumed relative stereochemistry and absolute configuration were confirmed by vibrational circular dichroism together with evaluation of the Hooft X-ray parameters. The molecular conformation is very similar in the gas stage and in the solid state. *Chirality 28:415–419, 2016.*

KEY WORDS: vibrational circular dichroism; single crystal X-ray diffraction; Hooft parameter; relative stereochemistry; absolute configuration

The structure of farinosin was originally proposed[1] as 4α-hydroxy-3-keto-8-eudesm-1,2-enolide based on some chemical transformations and mainly on a low-quality 60 MHz ^{1}H-NMR spectrum that was published in a book 5 years later.[2] The quality of the spectrum arose from the limited solubility of the natural product in chloroform in combination with the inherent low sensitivity of the NMR spectrometer. Regarding the stereochemistry, the authors assumed that the A/B ring junction was *trans* with the C-10 methyl group being *beta* oriented, and that the C-7/C-11 bond was also *beta* oriented. The original wrong structural assumption was almost instantaneously[3] corrected to **1** (Fig. 1) by moving the 4α-hydroxy group to the 11α position mainly based on reinterpretation of the same ^{1}H-NMR.

In another phytochemical study[4] involving **1**, which seemed to be the last one available, the occurrence of the natural product in hybrid plant material was discussed, but the assumptions regarding the relative stereochemistry and absolute configuration of **1** were not further addressed.

Over the years, farinosin (**1**) has turned out to be a biologically relevant molecule, as evidenced in studies on its antimicrobial activity[5] and on chemical ecology.[6–11] A couple of studies related to the active constituent abundances in botanical material containing **1** are also available.[12,13]

It follows that there is a need to complete the spectroscopic characterization of **1**, to know its relative stereochemistry, and to determine its absolute configuration, since nowadays such knowledge is of relevance to perform docking calculations that can lead to a better understanding of biological activities.

MATERIALS AND METHODS

General

The melting point was determined on a Fisher-Jhons apparatus and is uncorrected. All nuclear magnetic resonance (NMR) measurements were performed on a Varian (Palo Alto, CA) Mercury 300 spectrometer. Chemical shifts were referred to tetramethylsilane (TMS). Infrared (IR) and vibrational circular dichroism (VCD) spectra were obtained on a BioTools (Jupiter, FL) dual PEM Chiral*IR* FT-VCD spectrophotometer and optical rotations were measured on a Perkin-Elmer (Boston, MA) 341 polarimeter.

Plant Material

The aerial parts of *Encelia fariginosa* A. Gray var. *farinosa* A. Gray (Asteraceae) were collected some 9 km south of the city of Hermosillo, state of Sonora, Mexico, along Mexican federal highway number 15 (N 28° 56′, 48.7 , W 110° 57′ 43.4) at 225 m above average sea level on June 8, 2015. The plant material was identified by Dr. Jesús J. Sanchez Escalante at Herbario de la Universidad de Sonora, Sonora, Mexico, where a voucher sample, number 22656, is on deposit.

Extraction and Isolation

The air-dried leaves (277 g) were separated, powdered, packed in a glass column, and extracted by percolation with acetone (4 × 1 L). The solvent was evaporated under vacuum at 40°C to give 29.3 g of residue which was fractionated by column chromatography on Tonsil using hexanes, mixtures of hexanes-EtOAc of increasing polarity (7:3, 1 L; 3:2, 1 L; 1:1, 2 L; 2:3, 1 L and 1:4 1 L), and EtOAc. The fractions eluted with hexanes-EtOAc (1:1) were combined based on their thin-layer chromatography (TLC) profiles to give 13 g of residue. Crystallization from EtOAc-hexanes afforded 3.7 g of farinosin (**1**), mp 199–200° as colorless needles (lit.[1] colorless needles, mp 200–201° from $CHCl_3$-hexane), $[\alpha]_{589}$ -116, $[\alpha]_{578}$ -125, $[\alpha]_{546}$ -155, $[\alpha]_{436}$ -522 (*c* 1.0, $CHCl_3$), [lit.[1] $[\alpha]_{589}$ -111 (*c* 2.25, $CHCl_3$)], Of relevance is to note that we isolated **1** in 1.34% yield of dry leaves in contrast with the 0.13% yield reported[1] in the original study.

VCD Analysis

A sample of 6.0 mg of **1** dissolved in 150 μL of 100% atom-D $CDCl_3$ was placed in a BaF_2 cell with a path length of 0.2 mm and data were acquired with a resolution of 4 cm^{-1} over 20 h. A baseline correction was done by subtracting the spectrum of the solvent acquired under identical conditions. The sample stability was monitored by ^{1}H NMR analysis immediately before and after the VCD measurements.

*Correspondence to: Pedro Joseph-Nathan, Departamento de Química, Centro de Investigación y de Estudios Avanzados del Instituto Politécnico Nacional, Apartado 14-740, Mexico City, 07000 Mexico. E-mail: pjoseph@nathan.cinvestav.mx
Received for publication 6 January 2016; Accepted 12 February 2016
DOI: 10.1002/chir.22595
Published online 29 March 2016 in Wiley Online Library (wileyonlinelibrary.com).

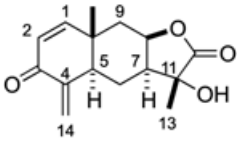

Fig. 1. Formula of farinosin (**1**).

Single Crystal X-Ray Diffraction Analysis of 1

The data were collected on a Bruker-Nonius (Billerica, MA) CAD4 diffractometer using Cu *Kα* radiation ($\lambda = 1.54184$ Å) at 293(2) K in the $\omega/2\theta$ scan mode. Crystal data were $C_{15}H_{18}O_4$, M = 262.29, orthorhombic, space group $P2_12_12_1$, $a = 6.4111(6)$ Å, $b = 10.8553(8)$ Å, $c = 19.867(4)$ Å, V = 1382.6(3) Å^3, Z = 4, $\rho = 1.260$ mg/mm^3, $\mu = 0.745$ mm^{-1}, total reflections 2279, unique reflections 1985 (R_{int} 0.01%), observed reflections 1969. The structure was solved by direct methods using the SHELXS-97 program included in the WinGX v1.70.01 crystallographic software package. For the structural refinement, the nonhydrogen atoms were treated anisotropically, and the hydrogen atoms, included in the structure factor calculation, were refined isotropically. The final R indices were [$I > 2\sigma(I)$] R1 = 3.0% and wR2 = 8.2%. Largest difference peak and hole, 0.156 and -0.100 e.Å^3. The Olex2 v1.1.5 software[14] allowed calculating the Hooft parameter[15,16] $y = 0.19(4)$. For the inverted structure that parameter was $y = 0.81(4)$. Crystallographic data (excluding structure factors) have been deposited at the Cambridge Crystallographic Data Centre. Copies of the data can be obtained free of charge on application to the CCDC, Cambridge, UK. The CCDC deposition number is 1457939.

Computational Methods

The atom coordinates extracted from the single crystal X-ray structure determination were used as the starting point to conduct conformational searches for **1**, using the molecular mechanics force field MMFF94 incorporated in the Compute*VOA* (BioTools) software package. Only two conformers within the first 10 kcal/mol were found, the second conformer being 7.94 kcal/mol above the lowest-energy conformer. Both conformers were submitted to geometry optimization, performing single point energy calculations at the B3PW91/6-31G(d,p) level of theory, followed by calculations using the same functional and the DGDZVP basis employing the Gaussian 09 W (Wallingford, CT) program. Since the relative energy obtained for these two conformers was significantly large, of 6.11 kcal/mol, only one conformer was further considered to calculate the vibrational frequencies, dipole transition moment, and rotational strengths. These data were then used to compute the IR and VCD spectra considering a sum of Lorentzian bands with half-widths of 6 cm^{-1}. Calculated and experimental spectra were contrasted using the Compare*VOA* software.[17] All Gaussian calculations were carried out in a server node with eight processors at 2.93 GHz and 8 Gb of RAM.

RESULTS AND DISCUSSION

Although the IR, UV, and mass spectroscopy (MS) data of farinosin (**1**) are well documented in the original publication,[1] the ^{1}H NMR data description is quite poor and, according to the time when the article was written, ^{13}C-NMR data measurements were nonexistent. Since **1** is a quite peculiar eudesmanolide, with four sp^2 carbon atoms at the A-ring and a very uncommon tertiary alcohol at the *γ*-lactone ring, the molecule deserves detailed ^{1}H and ^{13}C NMR characterization. Thus, inspection of the 300 MHz ^{1}H NMR spectrum allows doing a reasonable assignment that can then be improved by spectra iterations. The H-1 and H-2 vinyllic signals appear at δ 6.83 and 6.01, respectively, with $J_{1,2} = 10.0$ Hz, each signal showing a further long-range coupling, which for H-1 is $J_{1,6\alpha} = 0.7$ Hz and for H-2 is $J_{2,14E} = 0.8$ Hz, as evidenced by homonuclear spin decoupling. In turn, the exocyclic methylene group hydrogen atoms are also long-range coupled, since H-14*Z* appears at δ 6.15 as a doublet of doublets with $J_{5,14Z} = 2.3$ Hz and $J_{14E,14Z} = 1.0$ Hz, while H-14*E* appears at δ 5.25 as an apparent doublet of triplets with $J_d = 2.4$ Hz and $J_t = 1.0$ Hz since two coupling constant values are quite similar. The H-8 lactone ring closure signal appears as an apparent triplet of doublets at δ 5.06 with $J_t = 4.3$ Hz and $J_d = 2.0$ Hz since again two coupling constant values are quite similar. The allylic H-5 signal appears as an apparent doublet of quartets δ 2.58 with $J_d = 12.3$ Hz and $J_q = 2.3$ Hz, while the other methyne signal, corresponding to H-7, appears as a doublet of doublets of doublets at δ 2.36 with $J_{6\beta,7} = 12.6$ Hz, $J_{6\alpha,7} = 6.4$ Hz and $J_{7,8} = 4.0$ Hz. The two methylene groups at C-6 and C-9 also show individual signals for each hydrogen atom. The easiest one to be assigned is H-6*β* at δ 1.27 due to its axial nature, which renders it to seem as an apparent quartet with $J_q = 12.8$ Hz, since J_{gem} is of similar magnitude as the two *axial–axial* coupling constants. The other hydrogen atom of the same methylene group (H-6*α*) appears as a slightly broadened doublet of doublets of doublets at δ 1.85 with $J_{5,6\alpha} = 2.5$ Hz, $J_{6\alpha,6\beta} = 13.6$ Hz, and $J_{6\alpha,7} = 6.4$ Hz, since it is long-range coupled with H-1. The remaining methylene group shows H-9*β* at δ 2.39 as a doublet of doublets with $J_{8,9\beta} = 2.0$ and $J_{9\alpha,9\beta} = 15.6$ Hz, while H-9*α* appears at δ 1.76 as a slightly broadened doublet of doublets with $J_{8,9\alpha} = 4.6$ Hz and $J_{9\alpha,9\beta} = 15.6$ Hz, since it is long-range coupled with the angular methyl group, as is common in steroids[18] and as we recently evidenced during a 750 MHz ^{1}H-NMR study of 3*β*-acetoxypregna-5,16-dien-20-one.[19] The angular methyl group appears at δ 1.00 as a doublet with $J_{9\alpha,15} = 0.7$ Hz, which when irradiated causes sharpening of the H-9*α* signals at δ 1.76. In turn, the C-13 methyl group appears as a sharp singlet at δ 1.52 and the OH signal at δ 2.63 completes the picture.

The raw ^{1}H NMR data just discussed were used as the starting point to achieve a complete and detailed ^{1}H NMR assignment using the iterative full spin analysis that is integrated in the PERCH (PERCH Solutions, Kuopio, Finland) v. 2011.1 NMR software.[20] This methodology has been successful for the complete spectra assignment of several natural products,[21–23] and is based on the iterative minimization of the differences between the simulated and the experimental spectra to determine the total ^{1}H NMR data for the target molecule. The 300 MHz free induction decay of **1** was edited in the preparation (PAC) module, while the molecular structure of the minimum energy conformer was imported into the molecular modeling software (MMS) module, both of the PERCH shell. In addition, all chemical shift values and the already discussed coupling constants are introduced in the parameter table. With these values, iteration processes were accomplished until a convergence was reached to an RMS of 0.100%. All ^{1}H chemical shifts and coupling constants are summarized in Table 1. Since PERCH calculations afford chemical shift with six and coupling constants with four decimal places, and since the experimental 300 MHz spectrum was acquired with a magnet homogeneity better than 0.22 Hz, the chemical shifts and coupling constant values with three and two digits after a decimal point, respectively, given in Table 1 constitute a proper description, as has been done previously.[19,21–23] Comparison of the individual multiplets of the calculated and the experimental ^{1}H NMR spectra is shown in Figure 2.

With the detailed ^{1}H NMR assignments in hand, the ^{13}C NMR spectrum becomes relatively easy to be assigned. The two carbonyl groups at δ 188.7 and 176.7 follow directly from

TABLE 1. NMR Data (^{1}H, 300 MHz, ^{13}C, 75 MHz, $CDCl_3$) of farinosin (1).

position	^{13}C	^{1}H	multiplicity	*J*
1	159.61 d	6.825	dd	$^3J_{1,2}=9.91$, $^5J_{1,6\alpha}=0.70$
2	126.59 d	6.015	dd	$^3J_{1,2}=9.91$, $^5J_{2,14E}=0.77$
3	188.70 s	-	-	
4	144.46 s	-	-	
5	45.01 d	2.585	dddd	$^3J_{5,6\alpha}=2.53$, $^3J_{5,6\beta}=12.26$, $^4J_{5,14E}=2.44$, $^4J_{5,14Z}=2.25$
6	20.71 t	1.848(α)	dddd	$^5J_{1,6\alpha}=0.70$, $^3J_{5,6\alpha}=2.53$, $^2J_{6\alpha,6\beta}=-13.65$, $^3J_{6\alpha,7}=6.41$
		1.267(β)	ddd	$^3J_{5,6\beta}=12.26$, $^2J_{6\alpha,6\beta}=-13.65$, $^3J_{6\beta,7}=12.61$
7	45.46 d	2.360	ddd	$^3J_{6\alpha,7}=6.41$, $^3J_{6\beta,7}=12.61$, $^3J_{7,8}=4.02$
8	74.61 d	5.060	ddd	$^3J_{7,8}=4.02$, $^3J_{8,9\alpha}=4.63$, $^3J_{8,9\beta}=2.04$
9	37.32 t	1.763(α)	ddq	$^3J_{8,9\alpha}=4.63$, $^2J_{9\alpha,9\beta}=-15.57$, $^4J_{9\alpha,15}=0.72$
		2.395(β)	dd	$^3J_{8,9\beta}=2.04$, $^3J_{9\alpha,9\beta}=-15.57$
10	36.25 s	-	-	
11	77.46 s	-	-	
12	176.68 s	-	-	
13	19.08 q	1.522	s	
14	119.05 t	5.250(*E*)	ddd	$^5J_{2,14E}=0.77$, $^4J_{5,14E}=2.44$, $^2J_{14E,14}=0.96$
		6.152(*Z*)	dd	$^4J_{5,14Z}=2.25$, $^2J_{14,14Z}=0.96$
15	19.57 q	1.001	d	$^4J_{9\alpha,15}=0.72$

their chemical shifts, owing to the ketone at C-4 and the lactone at C-12, respectively, while the four remaining sp^2 carbon atoms are easily assigned from their *g*HSQC correlations, to the values given in Table 1. The same is true for all sp^3 carbon atoms, also summarized in the same table, since there are only one oxygen bearing and one nonoxygen bearing quaternary carbon atom that show no correlation in the *g*HSQC experiment.

Once the structure of **1** was confirmed after detailed ^{1}H and ^{13}C NMR measurements, we turned our attention to know its relative stereochemistry and absolute configuration (AC). Both were assumed for the original wrong structure, and were never evaluated in detail. For this purpose we undertook an X-ray study of the natural product. Since the molecule crystallized in the orthorhombic crystallographic system, a quarter of the reciprocal sphere data was collected, which contains twice the minimum reflections needed for a good structural solution. By doing so and using Cu *K*α radiation, the Hooft parameter[15,16] can in favorable cases be quite informative. Thus, a single crystal of **1** was mounted on an X-ray diffractometer equipped with a scintillation counter detector to get as precise as possible reflections and Cu *K*α monochromated radiation was used. The molecular structure was solved by direct methods and refined to a discrepancy index of 3.0%. These data were also used to calculate the Hooft parameter,[15,16] which was $y=0.19(4)$. For the inverted structure this parameter was $y=0.81(4)$, which suggests the correct enantiomer is the one depicted in Figure 3. In this case the Flack parameter was not very informative. Since the Hooft parameter is very conclusive only when for the correct enantiomer, the value is close to zero and for the wrong enantiomer it is close to the unit, we

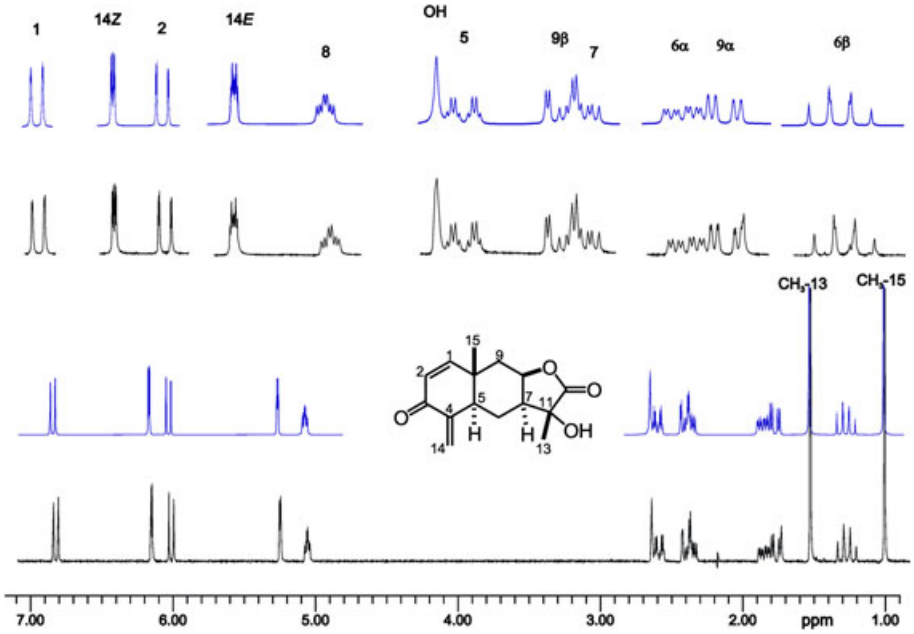

Fig. 2. Comparison of the PERCH calculated (top) and the experimental (bottom) ^{1}H NMR spectra of farinosin (**1**) in $CDCl_3$ at 300 MHz.

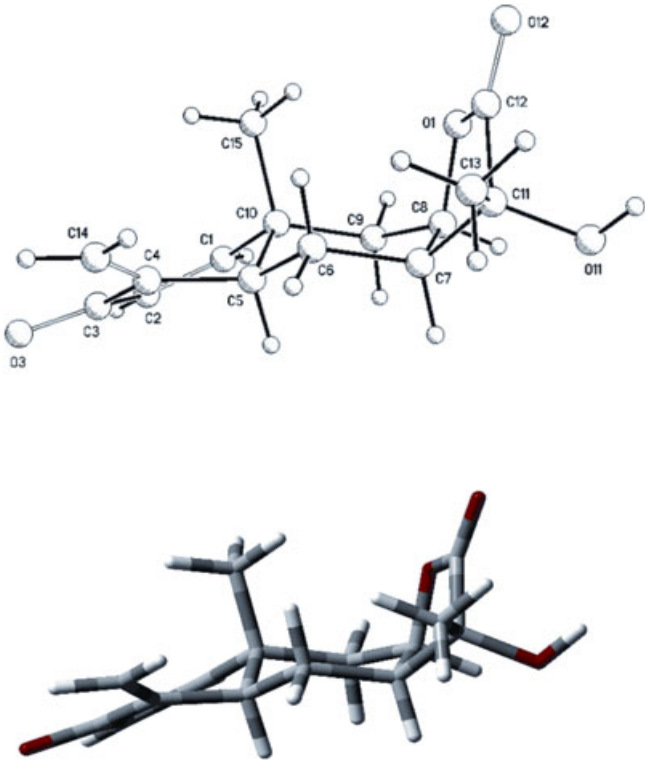

Fig. 3. X-ray crystal structure (top) and minimum energy conformation (bottom) of farinosin (**1**) at the B3PW91/DGDZVP level of theory.

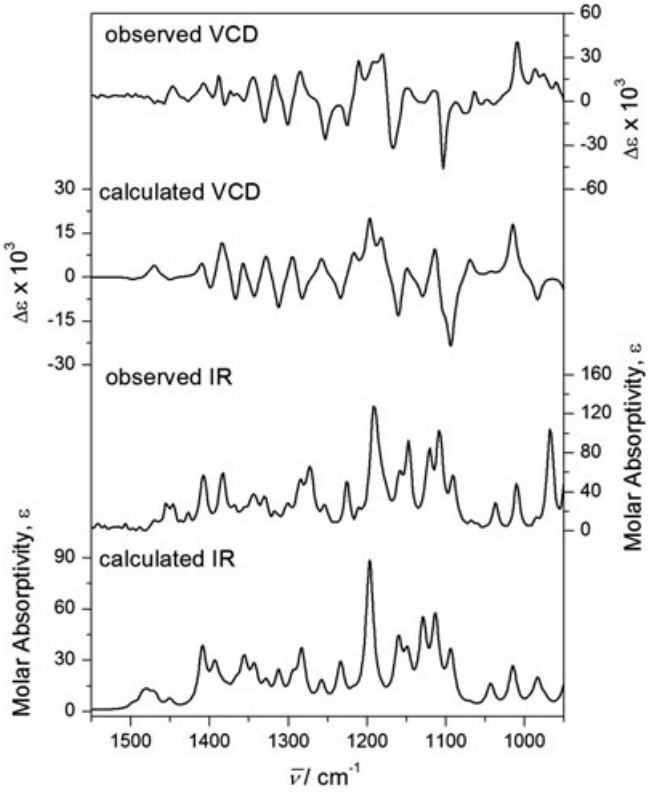

Fig. 4. Vibrational spectra of farinosin (**1**); calculations were done at the B3PW91/DGDZVP level of theory.

decided to obtain further independent conclusive evidence for the AC of **1** by VCD.

The VCD methodology has been applied successfully in recent years for the AC determination of a considerable number of natural products,[24–26] fundamentally by comparison of an experimental spectrum with one obtained by Density Functional Theory (DFT) calculations. Since farinosin (**1**) is not very soluble in chloroform, to obtain the experimental spectrum it was necessary to use a BaF_2 cell with a path length of 0.2 mm in combination with a long time for data acquisition, which in this case was 20 h. This combination of experimental conditions provided a good-quality VCD spectrum which can be compared with a calculated one.

For the calculation of the vibrational spectra it is necessary to determine the minimum energy conformational distribution of the studied molecule. For this purpose, the final atom coordinates generated by the X-ray analysis were used as the starting point in a Monte Carlo conformational search performed at the MMX level of theory, which provided two geometries with a relative energy of 7.94 kcal/mol. Geometry optimization of these two structures was carried out with DFT calculations using the functional B3PW91 and the DGDZVP basis set. With this quantum method the conformers had a relative energy of 6.11 kcal/mol, and therefore only the most stable conformer, depicted in Figure 3, was considered for computing the dipole transition moment and rotational strengths at the same level of theory. These values were extracted from the Gaussian output and processed using Lorentzian functions with a bandwidth of 6 cm^{-1}.

The assignment of the absolute configuration was followed by comparison of the experimental and calculated VCD spectra shown in Figure 4, and by using the Compare*VOA* software.[17] The program determines, using the IR data, a specific frequency scaling factor applied to the DFT calculated frequencies to bring them into better agreement with the observed frequencies, in this case 0.981. Other data provided[27] by the comparison software were the IR spectra similarity index (S_{IR}) = 94.8, the VCD spectra similarity for the correct (S_E) = 75.6, and the incorrect enantiomer (S_{-E}) = 24.0, the enantiomeric similarity index (*ESI*) = 51.6, and a 100% confidence level for the comparison.

The DFT optimized minimum energy conformer of **1** is almost identical to the solid state structure determined by X-ray diffraction, as can be seen in Figure 3. This is further evident from the fact that the largest difference of an angle of the two six-membered rings being 3.5° for H7-C7-C8-O, as can be observed in Table 2.

TABLE 2. Comparison of selected torsion angles (in deg.) of the X-ray structure and the most stable conformer of farinosin (1).

Angle	X-ray	DFT
H5-C5-C10-C15	-179.8	-179.8
H5-C5-C6-H6β	174.7	176.4
H6β-C6-C7-H7	166.6	163.6
H7-C7-C8-O	-156.4	-152.9
O-C8-C9-H9α	161.4	160.5
H9α-C9-C10-C15	-163.1	-165.0
C3-C2-C1-C10	0.2	2.9
C1-C2-C3-C4	-5.6	-7.4
C2-C3-C4-C5	- 20.9	-20.6
C2-C3-C4-C14	157.6	159.2
C3-C4-C5-C10	50.6	51.0
C4-C5-C10-C1	-52.2	-52.4

CONCLUSION

Although farinosin (**1**) was isolated as early as 1968, no detailed spectroscopic characterization of this very peculiar eudesmanolide is available in the literature. Therefore we completely assigned the ^{1}H NMR spectrum of the molecule, which includes the determination of all long-range coupling constants, and measured and assigned for the first time the ^{13}C NMR spectrum. We also determined the crystal X-ray structure, whose Hooft parameter suggested the absolute configuration, which in turn was tested by comparison of an experimental VCD spectrum with one obtained by DFT calculations at the B3PW91/DGDZVP level of theory. In addition, the calculated minimum energy conformation of **1** in the gas face is very similar to the solid state conformation determined by X-ray diffraction analysis.

ACKNOWLEDGMENTS

The authors are grateful to CONACYT-Mexico for financial support though grant number152994.

LITERATURE CITED

1. Geissman TA, Mukherjee R. Sesquiterpene lactones of *Encelia farinosa* Gray. J Org Chem 1968;33:656–660.
2. Yoshioka H, Mabry TJ, Timmermann BN. Sesquiterpene lactones: Chemistry, NMR and plant distribution. Tokyo: University of Tokyo Press; 1973. p 254.
3. Herz W, Subramaniam PS, Geissman TA. 3-Epiisotelekin from *Gaillardia aristata* Pursh, and the structure of farinosin. J Org Chem 1968;33: 3743–3749.
4. Bjeldanes LF, Geissman TA. Sesquiterpene lactones: Constituents of an F_1 hydrid *Encelia farinosa* X *Encelia californica*. Phytochemistry 1971;10:1079–1081.
5. Lee K-H, Ibuka T, Wu R-Y, Geisman TA. Structure-antimicrobial activity relationships among the sesquiterpene lactones and related compounds. Phytochemistry 1977;16:1177–1181.
6. Wisdom CS, Smiley JT, Rodriguez E. Toxicity and deterrency of sesquiterpene lactones and chromenes to the corn earworm (*Lepidoptera: Noctudiae*). J Econ Entomol 1983;76:993–998.
7. Wisdom CS. Use of chemical variation and predation as plant defenses by *Encelia farinosa* against a specialist herbivore. J Chem Ecol 1985;11:1553–1565.
8. Srivastava RP, Proksch P, Wray V. Toxicity and antifeedant activity of a sesquiterpene lactone from *Encelia* against *Spodoptera litoralis*. Phytochemistry 1990;29:3445–3448.
9. Srivastava RP, Proksch P. Insecticidal and antifeedant effect of compounds of plant origin against insect pests. Indian J Plant Protec 1993;21:234–239.
10. Kunze A, Mueller C, Proksch P. Chemical variation and defense of *Encelia farinosa*. Biochem Syst Ecol 1995;23:355–363.
11. Redak RA, Trumble JT, Paine TD. Interactions between the Encelia leaf beetle and its host plant *Encelia farinosa*: the influence of acidic fog on insect growth and plant chemistry. Environ Pollut 1997;95:241–248.
12. Wisdom CS, Rodriguez E. Quantitative variation of the sesquiterpene lactones and chromenes of *Encelia farinosa*. Biochem Syst Ecol 1982;10:43–48.
13. Wisdom CS, Rodriguez E. Seasonal age-specific measurements of the sesquiterpene lactones and chromenes of *Encelia farinosa*. Biochem Syst Ecol 1983;11:345–352.
14. Dolomanov O, Bourhis LJ, Gildea RJ, Howard JAK, Puschmann H. OLEX2: A complete structure solution, refinement and analysis program. J Appl Cryst 2009;42:339–341.
15. Hooft RWW, Straver LH, Spek AL. Using the *t*-distribution to improve the absolute structure assignment with likelihood calculations. J Appl Cryst 2010;43:665–668.
16. Hooft RWW, Straver LH, Spek AL. Determination of absolute structure using Bayesian statistics on Bijvoet differences. J Appl Cryst 2008;41:96–103.
17. Debie E, Gussem ED, Dukor RK, Herrebout W, Nafie LA, Bultinck P. A confidence level algorithm for the determination of absolute configuration using vibrational circular dichroism or Raman optical activity. ChemPhysChem 2011;12:1542–1549.
18. Bhacca NS, Williams DH. Applications of NMR spectroscopy in organic chemistry. Illustrations from the steroid field. San Francisco: Holden-Day; 1964. p 118.
19. Becerra-Martínez E, Ramírez-Gualito KE, Pérez-Hernández N, Joseph-Nathan P. Total ^{1}H NMR assignment of 3β-acetoxypregna-5,16-dien-20-one. Steroids 2015;104:208–213.
20. Laatikainen R, Tiainen M, Korhonen S-P, Niemitz M. Computerized analysis of high-resolution solution-state spectra. In: Harris RK, Wasylishen RE editors, Encyclopedia of magnetic resonance. Chichester, UK: Wiley; 2012. p 677–688.
21. Molina-Salinas GM, Rivas-Galindo VM, Said-Fernández S, Lankin DC, Muñoz MA, Joseph-Nathan P, Pauli GF, Waksman N. Stereochemical analysis of leubethanol, and anti-TB-active serrulatane from *Leucophyllum frutescens*. J Nat Prod 2011;74:1842–1850.
22. Villanueva-Cañongo C, Pérez-Hernández N, Hernández-Carlos B, Cedillo-Portugal E, Joseph-Nathan P, Burgueño-Tapia E. Complete ^{1}H NMR assignments of pyrrolizidine alkaloids and a new eudesmanoid from *Senecio polypodioides*. Magn Reson Chem 2014;52:251–257.
23. Alvarez-Cisneros C, Muñoz MA, Suárez-Castillo OR, Pérez-Hernández N, Cerda-García-Rojas CM, Morales-Ríos MS, Joseph-Nathan P. Stereospecific $^{5}J_{Hortho,OMe}$ couplings in methoxyindoles, methoxycoumarins, and methoxyflavones. Magn Reson Chem 2014;52:491–499.
24. Batista JM, Blanch EW, Bolzani VS. Recent advances in the use of vibrational chiroptical spectroscopic methods for stereochemical characterization of natural products. Nat Prod Rep 2015;32:1280–1302.
25. Joseph-Nathan P, Gordillo-Román B. Vibrational circular dichroism absolute configuration determination of natural products. In: Kinghorn AD, Falk H, Kobayashi J editors, Progress in the chemistry of organic natural products. Switzerland: Springer International Publishing 100;2015. p 311–451.
26. Burgueño-Tapia E, Joseph-Nathan P. Vibrational circular dichroism: Recent advances for the assignment of the absolute configuration of natural products. Nat Prod Commun 2015;10:1785–1795.
27. Burgueño-Tapia E, Zepeda LG, Joseph-Nathan P. Absolute configuration of (-)-myrtenal by vibrational circular dichroism. Phytochemistry 2010;71:1158–1161.